

1 | **Brief communication: Spatial and temporal variations in surface**
2 **snow chemistry along a traverse from coastal East Antarctica to the**
3 **ice sheet summit (Dome A)**

4
5 Guitao Shi^{1,2}, Hongmei Ma², Zhengyi Hu², Zhenlou Chen¹, Chunlei An², Su Jiang², Yuansheng Li²,
6 Tianming Ma², Jinhai Yu², Danhe Wang¹, Siyu Lu², Bo Sun², and Meredith G. Hastings³

7 ¹ Key Laboratory of Geographic Information Science (Ministry of Education), School of Geographic
8 Sciences and State Key Lab of Estuarine and Coastal Research, East China Normal University,
9 Shanghai 200241, China

10 ² Polar Research Institute of China, Shanghai 200062, China,

11 ³ Department of Earth, Environmental and Planetary Sciences and Institute at Brown for Environment
12 and Society, Brown University, Providence, Rhode Island 02912, USA.

13 *Correspondence to: G Shi (gtshi@geo.ecnu.edu.cn)

14

15 **Abstract**

16 To better understand snow chemistry in different environments across the Antarctic ice sheet, we
17 investigated snow ions on a traverse from coast to Dome A. Results show that the non-sea-salt (nss)
18 fractions of K^+ , Mg^{2+} , and Ca^{2+} are mainly from terrestrial particle mass, and nss Cl^- is associated with
19 HCl. Spatially, the proportions of non-sea-salt fractions of ions to the totals are higher in the interior
20 areas than on the coast, and seasonally, the proportions are higher in summer than in winter. Negative
21 nss SO_4^{2-} on the coast indicates sea salts from the sea ice, and marine biogenic emissions dominate
22 snow SO_4^{2-} in interior areas throughout the year. There is a large variability in environmental conditions
23 across the Antarctic ice sheet, and it is of significance to investigate the snow chemistry at as many
24 locations as possible and over time, given that the ice sheet itself, and precipitation and deposition
25 patterns and trends are changing. The China inland Antarctic traverse from coastal Zhongshan Station
26 to the ice sheet summit (Dome A) covers a variety of environments, allowing for a vast collection of
27 snow chemistry conditions across East Antarctica. Surface snow (the upper 3 cm, mainly representing
28 the summertime snow) and snow pit samples were collected on this traverse during five campaigns, to
29 comprehensively investigate the spatial and temporal variations in chemical ions (Cl^- , NO_3^- , SO_4^{2-} , Na^+ ,
30 NH_4^+ , K^+ , Mg^{2+} , and Ca^{2+}) and the related controlling factors. Results show that spatial patterns of ions
31 in surface snow are consistent among the five campaigns, with Cl^- , Na^+ , K^+ , and Mg^{2+} decreasing
32 rapidly with distance from the coast and NO_3^- showing an opposite pattern. No clear spatial trends in
33 SO_4^{2-} , NH_4^+ , and Ca^{2+} were found. In the interior areas, an enrichment of Cl^- versus Na^+ with respect to
34 seawater composition is ubiquitous as a result of the deposition of HCl, and nss Cl^- (nss, non-sea-salt
35 fraction) can account for up to 40 % of the total Cl^- budget, while nss K^+ and nss Mg^{2+} are mainly
36 associated with terrestrial particle mass. On average, nss Ca^{2+} and nss SO_4^{2-} in surface snow account for
37 77 and 95 % of total Ca^{2+} and total SO_4^{2-} , respectively. The high proportions of the non-sea-salt
38 fractions of Ca^{2+} and SO_4^{2-} are mainly related to terrestrial dust inputs and marine biogenic emissions,
39 respectively. Snow NH_4^+ is mainly associated with marine biological activities, with slightly higher
40 concentrations in summer than in winter. On the coast, parts of the winter snow are characterized with
41 negative nss SO_4^{2-} values, and a significant negative correlation between nss SO_4^{2-} and Na^+ in
42 wintertime snow was found, suggesting that sea salts originated from the sea ice. In the interior areas,
43 marine biogenic SO_4^{2-} still dominated snow SO_4^{2-} in winter, leading to significant positive nss SO_4^{2-}
44 values. Ion flux assessment suggests an efficient transport of nss SO_4^{2-} to at least as far inland as the
45 2800 m contour line.

带格式的

48 1 Introduction

49 Snow chemistry has been broadly investigated along traverses during the International
50 Trans-Antarctic Scientific Expedition (ITASE), e.g., DDU to Dome C, coast-interior traverse in Terre
51 Adelie, Syowa to Dome F, Terra Nova Bay to Dome C, 1990 ITASE, and US ITASE in West Antarctica
52 (Legrand and Delmas, 1985; Qin et al., 1992; Mulvaney and Wolff, 1994; Proposito et al., 2002;
53 Suzuki et al., 2002; Dixon et al., 2013), and Bertler et al. (2005) has comprehensively summarized the
54 glaciochemical data across the ice sheet, most of which are for surface snow. Among the major ions,
55 sea salt related ions (e.g., Na^+ and Cl^-), in general, are the most abundant species, and typically exhibit
56 a clear spatial trend, with concentrations falling off sharply with distance from the coast. ~~Acidic ions~~
57 ~~such as nitrate and sulfate (NO_3^- and SO_4^{2-}) are typically also abundant ionic species in snow, both of~~
58 ~~which can be deposited as salts in aerosols, and as gaseous acids. SO_4^{2-} in the snow is mainly from~~
59 ~~marine biogenic sulfur species, dimethylsulphide (DMS) (Legrand, 1995; 1997), with a small~~
60 ~~proportion from sea salt aerosols, while large volcanic eruption emissions can episodically contribute~~
61 ~~to spikes in SO_4^{2-} concentration (Legrand and Delmas, 1987; Jiang et al., 2012; Cole-Dai et al., 2013).~~
62 ~~Sources of NO_3^- are sometimes complicated to identify, due to the post-depositional processing after~~
63 ~~deposition into the snowpack (e.g., photolysis and volatilization) (e.g., Neubauer and Heumann, 1988),~~
64 ~~and stratospheric input and tropospheric transport from mid low latitudes have been proposed to be~~
65 ~~important sources (Legrand and Kirchner, 1990; Savarino et al., 2007; Lee et al., 2014; Shi et al.,~~
66 ~~2018a). As for calcium (Ca^{2+}) in snow, both long range transport of terrestrial particle mass and sea salt~~
67 ~~aerosols are important sources, and Ca^{2+} in ice cores recovered from interior areas is more likely~~
68 ~~associated with terrestrial inputs (e.g., Wolff et al., 2006). Terrestrial sources can also contribute to~~
69 ~~potassium (K^+) and magnesium (Mg^{2+}) in snow, but the contribution proportion varies significantly~~
70 ~~among sites (Legrand et al., 1988; Khodzher et al., 2014). In comparison with the other species,~~
71 ~~ammonium (NH_4^+) in snow has been rarely investigated due to the low concentration, and biogenic~~
72 ~~emissions in the Southern Ocean and/or mid latitude biomass burning were proposed to be the major~~
73 ~~sources, depending on the investigation sites (Legrand et al., 1999; Pasteris et al., 2014). In summary,~~
74 ~~source identification of ions in Antarctic snow and ice has been conducted intensely, however, the site~~
75 ~~and area-specific investigations are needed.~~

76 Temporally, Wwith varied sources and lifetimes, ions in snow often exhibit different seasonal
77 variations, e.g., sea salt related ions show high concentrations in winter, while elevated concentrations
78 of SO_4^{2-} and NO_3^- are frequently observed in summer (Neubauer and Heumann, 1988; Gragnani et al.,
79 1998; Traversi et al., 2004; Shi et al., 2015). ~~Indeed, these ions are frequently taken as seasonal markers~~
80 ~~for snow pit and ice core dating.~~ On annual to decadal time scales, ion concentrations in snow and ice
81 tend to be associated with changes in transport from year to year (Severi et al., 2009; Weller et al.,
82 2011), and thus large scale atmospheric and oceanic circulation in the Southern Hemisphere, ~~such as~~
83 ~~the Southern Annular Mode (SAM), Southern Oscillation (SO) and Southern Indian Ocean Dipole~~
84 ~~(SIOD),~~ could potentially influence variations in ions in ice snow and ice chemistry (Russell and
85 McGregor, 2010; Weller et al., 2011; Mayewski et al., 2017). ~~In addition, sea ice coverage around~~
86 ~~Antarctica plays an important role in variations in ions, and larger sea ice coverage is linked with~~
87 ~~higher sea salt concentrations, as well as non-sea salt SO_4^{2-} (nssSO_4^{2-}) concentrations in ice,~~
88 ~~particularly over glacial interglacial time scales (Kaufmann et al., 2010; Wolff et al., 2010; Abram et al.,~~
89 ~~2013). In addition to sources, lifetime, and transport processes, the preservation of ions are factors~~
90 ~~influencing concentrations in snow and ice, particularly the volatile species (e.g., NO_3^- and Cl^-).~~
91 ~~Post-depositional processes can result in significant losses of volatile species in snow, particularly at~~

92 sites with low snow accumulation rate (e.g., East Antarctic plateau) (Wagnon et al., 1999; Sato et al.,
93 2008; Shi et al., 2015).

94 In summary, spatial and temporal variations in snow chemistry are influenced by a variety of factors,
95 and further observations of ions in snow are needed to determine the controlling factors for particular
96 times and places. (Shi et al., 2015)

97 Although investigations of snow chemistry have been carried out along several overland traverses,
98 the investigation of snow chemistry under different environmental conditions and over time is needed,
99 given that the Antarctic ice sheet itself, and precipitation and deposition patterns and trends are
100 changing. The China inland Antarctic traverse from coastal Zhongshan Station to the ice sheet summit
101 (Dome A) covers a range of environments (~1250 km), e.g., high snow accumulation rate is present on
102 the coast and in some interior areas, and low accumulation rate is observed on the Dome A plateau, ~~and
103 thus provides further opportunity to investigate snow chemistry and its main controlling factors in
104 different environments.~~ Several investigations have been carried out to determine the concentrations
105 and spatial patterns of a few ionic species and trace elements on the traverse (e.g., Li et al., 2016; Du et
106 al., 2019), but limited snow chemistry data were previously available. ~~Additionally, the interannual
107 variations in snow chemistry and the related controlling factors on the traverse are far from understood.~~
108 Therefore, we used surface snow and snow pit samples collected during five China inland Antarctic
109 scientific expedition campaigns, to determine the spatial and temporal variations in a comprehensive
110 set of ions (Na^+ , NH_4^+ , K^+ , Mg^{2+} , Ca^{2+} , Cl^- , NO_3^- , and SO_4^{2-}) and their controlling factors. ~~This work
111 also presents data on snow chemistry from a less documented area, particularly at Dome A, providing
112 baseline values of snow ions and records of significance for evaluating potential changes in
113 atmospheric chemistry over Antarctica under a warming climate.~~

114 115 2 Methods

116 2.1 Sample collection

117 Snow samples were collected along the traverse from the coast to the ice sheet summit during five
118 Chinese National Antarctic Research Expedition (CHINARE) campaigns (Fig. S1). ~~In January 1999,
119 107 surface snow samples were collected on the traverse (from coast to the site ~1100 km from the
120 coast; the Chinese inland traverse coverage did not extend to Dome A then).~~ In January and February
121 in the years 1999, 2011, 2013, 2015, and 2016, 107, 120, 125, 117, and 125 surface snow samples were
122 collected on the traverse, respectively. In total, 594 snow samples were collected during the five
123 seasons. ~~For the snow sampling protocols refer to~~ Shi et al. (2018). It is noted that the surface ~3 cm
124 snow represents different lengths of time at different locations, considering the wide range of snow
125 accumulation rates on the traverse (Fig. 21(a)). At locations with high snow accumulation rate on the
126 coast, the upper 3 cm of snow may represent deposition from a few weeks ~~or a single snowfall~~, while
127 the surface 3 cm of snow could represent deposition over a few months on Dome A plateau. ~~Also, it is
128 possible that the upper 3 cm of snow can be representative of a single snowfall.~~ Still, the information
129 contained in the surface snow generally indicates summertime conditions, as the sampling took place
130 during late January and February in each season. ~~This allows for an investigation of summer snow
131 chemistry patterns on the traverse.~~

132 In addition to surface snow, snow pits were sampled in three representative areas on the traverse (~~P1,
133 P2, and P3; Fig. 1~~). P1, located on the coast (76.49 °E, 69.79 °S; 46 km from the coast), was sampled
134 in December 2015; P2, located in the interior area (77.03 °E, 76.42 °S; 800 km from the coast), was
135 sampled in January 2016; ~~and~~ P3, located on the Dome A plateau (77.11 °E, 80.42 °S; 1256 km from

136 the coast), was sampled in January 2010. Sites P1 and P2 are characterized with high snow
137 accumulation rate ($>100 \text{ kg m}^{-2} \text{ a}^{-1}$), while snow accumulation rate at P3 is $\sim 25 \text{ kg m}^{-2} \text{ a}^{-1}$. The depths
138 of P1, P2, and P3 are 180, 100, and 150 cm, respectively, with the respective sampling resolution of 5,
139 3, and 1 cm. ~~Details on the snow pit sampling are described in Shi et al. (2015). Snow pit samples were~~
140 ~~collected using the narrow mouth HDPE bottles pushed horizontally into the snow wall from the~~
141 ~~bottom of the pit and moving upwards.~~

142 ~~All of the bottles used for snow sampling were pre-cleaned with Milli-Q water (18.2 M Ω), dried in a~~
143 ~~class 100 super clean hood and then sealed in clean PE bags that were not opened until the field~~
144 ~~sampling started. During each sampling campaign, three pre-cleaned bottles filled with Milli-Q water~~
145 ~~taken to the field and treated to the same conditions as field samples represent field blanks. After~~
146 ~~collection, the bottles were again sealed in clean PE bags and preserved in clean expanded~~
147 ~~polypropylene boxes. All snow samples were transported and stored under freezing conditions (~ -20~~
148 ~~$^{\circ}\text{C}$).~~

149

150 2.2 Sample analysis

151 ~~Snow samples were first melted in the closed bottles on a super clean bench (class 100) before~~
152 ~~chemical measurements. In the class 100 room, about 5 ml of the melted sample was transferred to the~~
153 ~~pre-cleaned 8-ml ion chromatography (IC) autosampler vials, and then the lid was tightly screwed on to~~
154 ~~the vials. The samples were analyzed by an ICS-3000 IC system (Dionex, USA) IC for the~~
155 ~~concentrations of ions (Na^+ , NH_4^+ , K^+ , Mg^{2+} , Ca^{2+} , Cl^- , NO_3^- , and SO_4^{2-}). (Note that the IC was installed~~
156 ~~in a class 1000 clean room). The samples collected in 1999 were analyzed by using the DX 500 IC~~
157 ~~system (Dionex, USA), while the snow collected in the other campaigns were analyzed using an~~
158 ~~ICS-3000 IC system (Dionex, USA). The eluents for cations and anions were methanesulfonic acid~~
159 ~~(MSA) and potassium hydroxide (KOH), respectively. More details on this method ion determination~~
160 ~~are described in Shi et al. (2012). During sample analysis, replicate determinations ($n = 5$) were~~
161 ~~performed, and one relative standard deviation (1σ) for all eight ions was generally $<5\%$. In addition,~~
162 ~~the pooled standard deviation ($1\sigma_p$) of all replicate samples run in at least two different sets was~~
163 ~~examined ($n = 65$) and yielded 0.020, 0.023, 0.038, 0.022, 0.039, 0.005, 0.008, and 0.005 $\mu\text{eq L}^{-1}$ for~~
164 ~~Cl^- , NO_3^- , SO_4^{2-} , Na^+ , NH_4^+ , K^+ , Mg^{2+} , and Ca^{2+} , respectively.~~

165 In Antarctic snow, previous observations suggested that concentrations of H^+ can be reasonably
166 deduced from the ion-balance disequilibrium, ~~if the direct measurements of H^+ are unavailable~~
167 ~~(Legrand and Delmas, 1985; Legrand, 1987). Here, H^+ concentration is calculated as follows.~~

168 $[\text{H}^+] = [\text{SO}_4^{2-}] + [\text{NO}_3^-] + [\text{Cl}^-] - [\text{Na}^+] - [\text{NH}_4^+] - [\text{K}^+] - [\text{Mg}^{2+}] - [\text{Ca}^{2+}]$ Eq. (1),

169 where ion concentrations are in $\mu\text{eq L}^{-1}$. In addition, the non-sea-salt fractions of ions (nssX), including
170 nssCl⁻, nssSO₄²⁻, nssK⁺, nssMg²⁺, and nssCa²⁺, can be calculated from the following expression,

171 $[\text{nssX}] = [\text{X}]_{\text{snow}} - ([\text{X}]/[\text{Na}^+]_{\text{seawater}}) \times [\text{Na}^+]_{\text{snow}}$ Eq. (2),

172 where [X] is the concentration of ion X, and [X]/[Na⁺] ratios in seawater are 1.17 (Cl⁻), 0.12 (SO₄²⁻),
173 0.022 (K⁺), 0.23 (Mg²⁺) and 0.044 (Ca²⁺) (in $\mu\text{eq L}^{-1}$). ~~The values of nssX are identical to the~~
174 ~~concentrations in excess with respect to the seawater composition in previous observations (e.g.,~~
175 ~~Legrand and Delmas, 1985).~~

176

177 2.3 Principal component analysis (PCA) of ions

178 ~~The essence of PCA is converting the observed variables into factors or principal components, so~~
179 ~~that a minimized set of underlying variables can be identified. Bartlett sphericity test and~~

180 Kaiser-Meyer-Olkin test indicated that the raw data (i.e., ion concentrations in surface snow) were
181 suitable for PCA ($p < 0.001$). Varimax with Kaiser normalization rotation was applied to maximize the
182 variances of the factor loadings across variances for each factor. The regression method was selected
183 for calculating the factor score coefficient. Three components with eigenvalue > 1.0 were extracted. The
184 loadings were obtained from the eigenvalues of the three components and their corresponding
185 eigenvectors.

186 Because the samples collected in 1999 did not cover the whole traverse and the ion concentrations
187 were determined using a different IC system, the ion data of 1999 were excluded in the PCA analysis in
188 the following.

189 (Bertler et al., 2005; Shi et al., 2015)

192 3 Results

193 3.1 Chemical ion variations in snow pits

194 Clear seasonal cycles of Na^+ and nssSO_4^{2-} are present in P1 and P2, and thus the two pits can be well
195 dated, spanning ~ 3 years (Figs. 3 (a) and (b) Fig. S2). Based on the snow pit dating, it is estimated that
196 snow accumulation rate is ~ 50 (P1) and ~ 33 cm snow per year (P2), agreeing well with the field
197 measurements (P1: $\sim 150 \text{ kg m}^{-2} \text{ a}^{-1}$; P2: $\sim 100 \text{ kg m}^{-2} \text{ a}^{-1}$; Fig. 2(a)), assuming a snow density of $\sim 0.33 \text{ g}$
198 cm^{-3} . At P1, negative nssSO_4^{2-} values are observed in winter snow, i.e., $\text{SO}_4^{2-}/\text{Na}^+$ ratio below that of
199 bulk seawater, while all of the nssSO_4^{2-} data in P2 pit are positive. It is difficult to assign the samples in
200 the snow pits to the four distinct seasons based on the measured parameters, and thus, in the following
201 discussion, we choose a conservative assignment method, i.e., a summer season featured with higher
202 nssSO_4^{2-} and $\text{SO}_4^{2-}/\text{Na}^+$ ratio (and lower Na^+) and a winter season characterized with the opposite
203 patterns. In addition to SO_4^{2-} and Na^+ , the other species also show seasonal variations, especially in
204 pit in P1, where elevated levels of NO_3^- and NH_4^+ are generally present in summer snow, and the values
205 concentrations of Cl^- , K^+ , Mg^{2+} , and Ca^{2+} are high in winter. It is noted that even in the same season,
206 ion concentrations could vary among samples at a single site (e.g., shaded areas in Figs. 3(a) and (b)).
207 As for nssSO_4^{2-} at P3, the very large signal at the depth of ~ 120 cm is most likely the fallout from the
208 massive eruption of Pinatubo in 1991 (Fig. S2 Fig. 3(e)), based upon previous observations at Dome A
209 (e.g., Hou et al., 2007). Based on nssSO_4^{2-} signals and the method proposed by Cole-Dai et al. (1997),
210 49 continuous samples have been identified as influenced by Pinatubo eruption, covering ~ 2.5 years,
211 possibly suggesting that the effects of Pinatubo eruption on atmospheric chemistry lasted at least for
212 2.5 years over Dome A. Interestingly, it is noted that only elevated SO_4^{2-} concentrations are present
213 during this period, and anomalous high or low concentrations of other ions are absent. Additionally, no
214 correlation was found between nssSO_4^{2-} and other species during the 2.5 years, possibly suggesting that
215 Pinatubo volcanic emissions contribute less to the ion budgets other than SO_4^{2-} at Dome A. Previous
216 investigations proposed that Na^+ and nssSO_4^{2-} in surface snow (top 1 cm) collected during a full year
217 at central Antarctica show clear seasonal cycles, with high (low) Na^+ in winter (summer) snow (Udisti
218 et al., 2012). At P3, Na^+ , nssSO_4^{2-} and the ratios of $\text{SO}_4^{2-}/\text{Na}^+$ fluctuate significantly (Fig. 3(e)), and
219 these contrasts are unlikely indicative of the seasonal cycles as that for P1 and P2. In a full year of
220 snow accumulation at P3, on average, about 7–8 samples were collected, allowing for examining the
221 seasonal variability of ions. Following the field measurements of snow accumulation rate at Dome A
222 during 2008–2011 ($\sim 20 \text{ kg m}^{-2} \text{ a}^{-1}$; Ding et al., 2015), the snow samples covering the years 2008 and
223 2009 can be roughly identified, assuming an even distribution of snow accumulation throughout the

带格式的：字体颜色：红色

224 year. In total, there are 7 and 8 samples identified in the years 2008 and 2009, respectively (Fig. S1),
225 and no seasonal cycles in Na^+ , nssSO_4^{2-} , and $\text{SO}_4^{2-}/\text{Na}^+$ ratio were found due to the low snow
226 accumulation rate at P3. In addition, the post depositional processes (e.g., migration, diffusion, and
227 ventilation processes) and/or wind scouring can obscure the original signal, resulting in the absence of
228 seasonal cycles of ions at P3.

229 In terms of the non-sea-salt fractions in snow pits, nssCl^- is lower at P1 ($0.25 \pm 0.28 \mu\text{eq L}^{-1}$) than at
230 the inland sites P2 and P3 (0.42 ± 0.18 and $0.58 \pm 0.34 \mu\text{eq L}^{-1}$, respectively), while the concentrations of
231 nssK^+ , nssMg^{2+} , and nssCa^{2+} generally show a similar spatial patterns, possibly due to the low snow
232 accumulation rate in interior areas. Different from the sea salt ions and nssSO_4^{2-} In general, nssCl^- ,
233 nssK^+ , nssMg^{2+} , and nssCa^{2+} in pits P1 and P2 snow pits, do not show significant clear seasonal
234 patterns/cycles. In the coastal pit P1, the non-sea salt fractions account for less (< 30%) of the total
235 ions, and the contribution percentages of non-sea-salt fractions increased at inland sites P2 and P3,
236 about 30-70%.

237

238 3.2 Ion concentrations in surface snow

239 Concentrations of ions in surface snow collected during the five seasons are shown in Fig. 21, and
240 the ranges (mean) of Cl^- , NO_3^- , SO_4^{2-} , Na^+ , NH_4^+ , K^+ , Mg^{2+} , and Ca^{2+} are 0.15-14.6 (1.29), 0.48-12.6
241 (3.37), 0.37-5.63 (1.52), 0.09-12.74 (0.68), 0.04-0.77 (0.16), 0.01-0.27 (0.04), 0.11-2.76 (0.22), and
242 0.01-0.50 (0.13) $\mu\text{eq L}^{-1}$, respectively. These values generally fall within the reported ranges of the
243 ITASE program sampling (Bertler et al., 2005). Ion concentrations are both spatially and temporally
244 variable, with the coefficient of variation (ratio of one standard deviation over mean) of >0.48,
245 suggesting a large variability across the traverse. In general, ion concentrations do not follow a normal
246 distribution ($p > 0.05$, One-Sample Kolmogorov-Smirnov Test), with the values of skewness and
247 kurtosis above 1.0, but they correspond to a logarithmic normal distribution. Spatially, Cl^- , Na^+ , K^+ , and
248 Mg^{2+} show very high concentrations within the narrow coastal region, and decrease sharply further
249 inland, with minimum values on the Dome A plateau (>~1000 km from the coast). It is noted that some
250 samples on the coast also show elevated Ca^{2+} concentrations. The high ion concentrations near the
251 coast may be associated with the strong marine air mass intrusions (Hara et al., 2014). NO_3^- shows an
252 opposite spatial trend, with increasing values towards inland. As for SO_4^{2-} (and nssSO_4^{2-}), NH_4^+ , and
253 Ca^{2+} , no clear spatial trend was found.

254 Among the chemical ions in surface snow, the most abundant species is H^+ , accounting for 30-40 %
255 of the total ions, followed by NO_3^- , SO_4^{2-} , and Cl^- . In general, NH_4^+ , K^+ , Mg^{2+} , and Ca^{2+} are the smallest
256 component of the ionic composition, with the four cation summing to (6.0 ± 3.4) % of the total (Fig. S3).

257 pH values of surface snow sampled in 2013 were measured with a glass pH electrode in a class 100
258 room at room temperature (-20°C), and H^+ concentrations deduced from pH are correlated well with
259 the values calculated from the ion-balance method (Fig. 4(a)). On average, H^+ concentrations obtained
260 from the ion-balance approach are 25 % lower than those deduced from pH. It is noted that pH
261 measurements in this study remain uncertain considering that snow samples are highly undersaturated
262 with respect to carbon dioxide (CO_2) immediately after melting in the lab. On the other hand, organic
263 acids, e.g., monocarboxylic and methanesulfonic acids (MSA), were excluded in H^+ calculation (Eq. 1),
264 although their concentrations in Antarctic snow tend to be very low. If the contribution of organic acids
265 to H^+ in snow is negligible, the x-intercept of $-2.4 \mu\text{eq L}^{-1}$ in the linear regression (Fig. 3(a)) can be
266 regarded as the contribution from dissolved CO_2 in snow during pH measurements. This value is close
267 to that of pure water in equilibrium with CO_2 in the atmosphere, with $\text{pH}=5.6$ corresponding to H^+

268 concentration of $2.5 \mu\text{eq L}^{-1}$. Here, the calculated H^+ concentrations vary in the range of $0.51\text{--}10.01$
269 $\mu\text{eq L}^{-1}$, with a mean of $3.53 \pm 1.61 \mu\text{eq L}^{-1}$. In general, the calculated H^+ values of the coastal surface
270 snow are generally comparable to previous direct measurements in Terre Adelie.

271 272 3.3 Spatial patterns of ions in surface snow

273 The spatial distribution patterns of ions on the traverse are consistent among the five campaigns (Fig.
274 2). In general, Cl^- , Na^+ , K^+ , and Mg^{2+} show very high concentrations within the narrow coastal region,
275 and decrease sharply further inland, with low values on Dome A plateau ($\sim 1000\text{--}1250$ km from the
276 coast). It is noted that some samples on the coast also show elevated Ca^{2+} concentrations. The spatial
277 patterns are consistent with previous observations, and the high ion concentrations near the coast have
278 been explained by the strong marine air mass intrusions.

279 Different from other species, NO_3^- concentrations near the coast are low, and increase towards inland,
280 with the highest values on the Dome A plateau. A significant correlation is found between NO_3^- and
281 distance from the coast, with $r = 0.56$ and $p < 0.001$. The spatial trend of NO_3^- is generally opposite to
282 that of snow accumulation rate on the traverse (Figs. 2(a) and (e)), possibly associated with
283 post-depositional cycling of NO_3^- in surface snow. Similarly, there is a close relationship between H^+
284 and distance from the coast ($r = 0.48$, $p < 0.001$), suggesting a higher acidity of inland snow. As for
285 SO_4^{2-} (and nssSO_4^{2-}), NH_4^+ , and Ca^{2+} , no clear spatial trend was found on the traverse.

286 It is noted that the surface snow mainly represents the summertime deposition (section 2.1), and
287 therefore the spatial patterns of ions here can only indicate summertime conditions. In addition, the
288 spatial variations of ions in surface snow may arise from the temporal changes in chemical ions,
289 considering that the upper ~ 3 cm corresponds to deposition over different time at varied locations.

290 Previous investigations of ions in surface snow covered various depths among different traverses or
291 campaigns, e.g., 1.0 m deep layer for the traverse from Terra Nova Bay to Dome C and top 25 cm snow
292 for the 1990 ITASE. It is noted that different sampling depths can result in varied ion concentrations in
293 snow. For instance, in inland Antarctica, NO_3^- is often concentrated on the top few centimeter snow,
294 and decreases significantly with increasing depth. Thus, any comparison of ion concentrations in
295 surface snowpack collected from different campaigns should be made with caution.

296 The percentages of each constituent to the total ions in surface snow on the traverse are shown in
297 Figs. 4(b)–(d). The most abundant species is H^+ , accounting for about 30–40 % of the total ions,
298 followed by NO_3^- , SO_4^{2-} , and Cl^- . In general, ions NH_4^+ , K^+ , Mg^{2+} , and Ca^{2+} are the smallest component
299 of the ionic composition, with the four cation summing to ~ 5 % of the total. Spatially, the contribution
300 percentages of H^+ and NO_3^- increase with increasing distance from the coast, with the highest values on
301 Dome plateau (42.3 and 34.5 %, respectively), while Cl^- , Na^+ , Mg^{2+} , and NH_4^+ show an opposite
302 pattern and no clear trend was observed for SO_4^{2-} . The high contribution percentage of H^+ is consistent
303 with previous investigations, and suggests acidic characteristics of summertime surface snow.

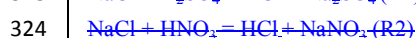
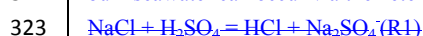
304 (Bertler et al., 2005; Erbland et al., 2013)

305 306 4 Discussions

307 4.1 Non-sea-salt fractions of ions in surface snow

308 The positive (negative) nssX values indicate the enrichment (depletion) of an ion with respect to the
309 seawater composition. In surface snow, the non-sea-salt fractions of Cl^- , SO_4^{2-} , K^+ , Mg^{2+} , and Ca^{2+} are
310 0.51 ± 0.44 , 1.44 ± 0.84 , 0.03 ± 0.02 , 0.08 ± 0.06 , and 0.09 ± 0.08 , respectively. In the following, we will
311 discuss the non-sea-salt fractions of ions in surface snow by plotting the ions versus Na^+ .

312 Correlation plots of ions versus Na^+ in surface snow are shown in Fig. 52, and the plots above
313 (below) the seawater dilution line represent the enrichment (depletion) of the ions. The further the plots
314 deviate away from the line, the higher degree of enrichment or depletion of the ions. On the coast, most
315 of the Cl^-/Na^+ data are distributed close to the seawater dilution line (Fig. 22(a)), indicating a
316 quantitative sea salt tracer of snow Cl^- , while most of the plots in the interior areas are above the
317 seawater line, suggesting an enrichment of snow Cl^- . On this traverse, nss Cl^- accounted for an average
318 of 38 (39±24) % of total Cl^- on the traverse, with lower (higher) percentages values on the coast
319 (plateau in the interior areas), generally in line with previous reports (e.g., Suzuki et al., 2002). The
320 elevated fractions of nss Cl^- are likely associated with the 'secondary' HCl which is produced by the
321 reactions between sea salts and acids (e.g., HNO_3 and H_2SO_4). The modifications in Cl^- with respect to
322 bulk seawater can occur via the heterogeneous reactions, as follows (Finlayson-Pitts, 2003).



325 In the atmosphere, the production of HCl will result in depletion of Cl^- in sea salt aerosol. The
326 'secondary' HCl , in the gas phase and/or fine aerosol mode, can be transported further inland due to the
327 longer lifetime (versus the coarse sea salt aerosols removed preferentially from the atmosphere). In this
328 case, an enrichment of Cl^- would be expected in the inland snowpack. On the other hand, Cl^- is not
329 irreversibly deposited to the snow, and it can be released back into the atmosphere through the
330 formation of HCl , resulting in an enrichment of Cl^- in surface snow via re-deposition. Post-depositional
331 losses of HCl are thought to be associated with snow accumulation rate, with larger losses occurring at
332 sites with snow accumulation generally $< 40 \text{ kg m}^{-2} \text{ a}^{-1}$. Indeed, a negative correlation was found
333 between snow accumulation and nss Cl^- (Fig. 6(a)) for most interior areas that featured low snow
334 accumulation and consequently an enhanced cycling of Cl^- .

335 Different from Cl^- , Mg^{2+} is irreversibly deposited into the snow. Most of the $\text{Mg}^{2+}/\text{Na}^+$ data points
336 are above or close to the seawater dilution line, similar to that of Cl^-/Na^+ (Fig. 2(d)). On the coast,
337 $\text{Mg}^{2+}/\text{Na}^+$ data points are in general close to the seawater dilution line, suggesting the main source is
338 sea salt aerosols, while most of the inland samples are slightly enriched with Mg^{2+} , agreeing with
339 previous observations (e.g., Dome F; Hara et al., 2014), and the fraction of nss Mg^{2+} , on average,
340 represents (44±19) % of Mg^{2+} in snow, with lower (higher) values on the coast (plateau) (Fig. 2(d)).
341 The enrichment of Mg^{2+} has not been observed in sea salt particles produced by bubble bursting (Keene
342 et al., 2007), and thus enriched Mg^{2+} in the snow is unlikely associated with sea salt spray. In the
343 atmosphere, sea salt aerosols would can also be modified at low temperatures via the formation of
344 mirabilite, thus leading to an elevated ratio of $\text{Mg}^{2+}/\text{Na}^+$ if mirabilite precipitates from the aerosols.
345 However, the solid-liquid separation of mirabilite in the aerosol droplet was not observed in the
346 experiments (Wagenbach et al., 1998). Thus, the enrichment of Mg^{2+} in surface snow is unlikely
347 associated with sea salt fractionation. Although it is proposed that Mg^{2+} separation in sea salts can
348 occur in surface snow due to the re-freezing process on surface snow (i.e., the quasi-liquid layers on the
349 crystal surface can act like seawater freezing; Hara et al., 2014), our measurement of Mg^{2+} in bulk
350 snow is unlikely to support this process responsible for Mg^{2+} enrichment. A previous observation
351 conducted near this traverse showed a moderate correlation of Mg^{2+} with element Al in the surface
352 snowpack ($r=0.53$, $p<0.05$), indicating a contribution of continental dust (Khodzher et al., 2014). Thus,
353 the most plausible interpretation of enriched nss Mg^{2+} in surface snow is the contribution of terrestrial
354 aerosols.

355 Similar to Mg^{2+} , most of K^+/Na^+ data points are close to the seawater dilution line on the coast,

带格式的：缩进：首行缩进： 2 字符

356 suggesting a primary contribution of sea salt spray (Fig. 52(c)). Slightly enriched K^+ was present is
357 ubiquitous in inland snow interior areas, possibly indicating other sources such as associated with
358 biological activity on the coast, mineral transport, and combustion emissions in the Southern
359 Hemisphere (Virkkula et al., 2006; Hara et al., 2013). Note that the all sampling sites are at least
360 several tens of kilometers away from the coast, the contribution of biological activity to snow K^+ would
361 be rather minor (Rankin and Wolff, 2000). A lack of correlation between K^+ (or $nssK^+$) and refractory
362 black carbon (rBC, unpublished data; Fig. S4), which mainly represent the biomass burning emissions
363 in the Southern Hemisphere (Sigl et al., 2016), suggests that K^+ in surface snow is unlikely dominated
364 by biomass burning emissions. A previous investigation of the atmospheric particles—

365 Positive $nssCa^{2+}$ is generally present on the traverse, with most of the Ca^{2+}/Na^+ data points above the
366 seawater dilution line, especially at inland sites (Fig. 5(e)). The fraction of $nssCa^{2+}$, on average,
367 accounts for (73 ± 26) % of total Ca^{2+} in surface snow, with high percentages in the interior areas,
368 indicating other dominant sources. In Antarctica, snow $nssCa^{2+}$ has been was thought to be mainly
369 associated with terrestrial inputs, possibly from both South America and Australia (Bertler et al., 2005;
370 Wolff et al., 2010). (Bertler et al., 2005; Wolff et al., 2010; Du et al., 2018). Previous modeling studies
371 suggest that the dust mass reaching East Antarctica mainly originates from South America, specifically
372 Patagonia (Basile et al., 1997; Wolff et al., 2006; Mahalinganathan and Thamban, 2016). Metal
373 isotopes in snow collected on this traverse suggested that Australian mineral dust also can contribute to
374 snow particles (Du et al., 2018). In addition, Antarctic ice free areas were thought to be a contribution
375 to snow dust (Delmonte et al., 2013; Du et al., 2018). If the dust mass originated from ice free area near
376 the coast and dominated $nssCa^{2+}$, then $nssCa^{2+}$ concentrations near the coast would be expected to be
377 higher, while the data shows the opposite. Thus, terrestrial dust mass, possibly from both South
378 America and Australia likely dominates snow $nssCa^{2+}$. It is noted that some Ca^{2+} concentrations in
379 surface snow (e.g., coastal and some inland sites) are above $0.2 \mu\text{eq L}^{-1}$ (Fig. 2(i)), slightly higher than
380 most reports of snow and ice under present day climate. On the coast, the high concentrations could be
381 related to marine inputs, while the elevated values in the inland regions (about 500-900 km from the
382 coast, where the glaze/dune are distributed) are possibly associated with the low and fluctuating snow
383 accumulation rate due to the strong wind scouring. Similarly, in the glaze/dune regions on the US
384 ITASE traverses across East and West Antarctica, concentrations of Ca^{2+} in snow and ice are also often
385 above $0.2 \mu\text{eq L}^{-1}$.

386 Positive $nssSO_4^{2-}$ is present in all surface snow (Fig. 5(b)), together with the minimum sea ice
387 coverage around East Antarctica in late summer (Holland et al., 2014), suggesting that sea salts in
388 surface snow are from open seawater rather than from the sea ice. On the traverse, $nssSO_4^{2-}$ represents
389 (94 ± 5) % of total SO_4^{2-} in surface snow, with lower (higher) proportions on the coast (plateau) (Fig.
390 2(b)), suggesting a dominant role of marine bioactivities. In Antarctica, $nssSO_4^{2-}$ essentially originates
391 from marine biogenic production of DMS and occasionally from explosive volcanism. In this study, the
392 significant enrichment of SO_4^{2-} suggests a dominant role of ocean bioactivities. Different from the
393 coarse sea salt aerosols, $nssSO_4^{2-}$ originating from marine biogenic production of DMS can form fine
394 aerosol particles in the atmosphere (Legrand et al., 2017a), resulting in long atmospheric residence time
395 (>10 days to weeks) and consequently efficient transport (Bondietti and Papastefanou, 1993; Hara et al.,
396 2014). This can help explain the elevated deposition flux of $nssSO_4^{2-}$ frequently found at inland
397 Antarctic sites, e.g., site P2 (discussed below). On this transect, a negative relationship was found
398 between snow accumulation rate and SO_4^{2-} (or $nssSO_4^{2-}$) (Figs. 6(e) and (d)), suggesting that snow
399 accumulation rate can influence snow SO_4^{2-} concentration, possibly via dilution effects, but overall

带格式的：缩进：首行缩进： 1.5 字符

400 <10 % of the variation in SO_4^{2-} concentrations can be explained by the relationship.

401
402 (Guo et al., 2020) The ternary diagram of Cl^- , Na^+ , and SO_4^{2-} can well characterize the modification
403 processes to sea salt aerosols, and the ternary plot of the three ions in surface snow is shown in Fig. 7.
404 The values of the ions were normalized via the following equation,—

405
$$X = [X] / ([\text{Na}^+] + [\text{Cl}^-] + [\text{SO}_4^{2-}]) \text{ Eq. (3)}$$

406 where $[X]$ is the concentration of ion X in the snow (in $\mu\text{eq L}^{-1}$). The dashed line between the seawater
407 reference value and the SO_4^{2-} vertex represents the sea salt aerosol composition with additional SO_4^{2-} ;
408 i.e., the ratio of Cl^-/Na^+ keeps constant (1.17) with additional SO_4^{2-} along the dashed line. The presence
409 of acids (HNO_3 and H_2SO_4) would result in the liberation of HCl into the atmosphere via reactions R1
410 and R2, resulting in the changes in Cl^-/Na^+ ratios, i.e., either Cl^- loss or gain are located right or left of
411 the line, respectively. It is shown that all of the data points are above the seawater plot, suggesting an
412 enrichment of SO_4^{2-} in surface snow. Most of the data points are located left of the line, indicating the
413 general enrichment of Cl^- due to reactions R1 and R2 occurring in the atmosphere and/or in the
414 snowpack. But the coastal data points are generally close to the line, suggesting that the degree of sea
415 salt modification is generally low in the snow.

416 417 4.2 Groups of ions in surface snow

418 PCA is a powerful tool for identifying the common sources and/or transport process of chemicals in
419 different environments. The PCA results (i.e., loadings in each PC), communalities, initial eigenvalues,
420 and explained cumulative percent of the ions in surface snow are listed in Table 1. The first three PCs
421 accounted for 76 % of the variation of the eight original variables. PC1 accounts for 46 % of the
422 variance and is highly loaded by Cl^- , Na^+ , K^+ , and Mg^{2+} , with the factor loadings higher than 0.7. In
423 addition, the four species are correlated well with each other (Table 2), suggesting the variation of the
424 four species is dominated by sea salt aerosols. PC2 accounts for 17 % of the total variance, and the
425 loading values of NH_4^+ and Ca^{2+} in PC2 are high, -0.8. Ca^{2+} is mainly from terrestrial particle mass,
426 while NH_4^+ is thought to be mainly associated with biological decomposition of organic matter in the
427 Southern Ocean. In addition, biomass burning from mid-latitudes can contribute to snow NH_4^+ at some
428 sites, and the penguin colony emissions can be important inputs to NH_4^+ in snow several km from the
429 colony. On this traverse, no correlation was found between NH_4^+ and biomass burning tracers (e.g.,
430 black carbon and phenolic compounds) in surface snow, suggesting a minor role of biomass burning
431 emissions. Thus, the high NH_4^+ concentrations on the coast are likely associated with marine biogenic
432 emissions. In this case, it is possible that a similar transport pathway can explain, at least in part, the
433 positive loadings of both NH_4^+ and Ca^{2+} in PC2.

434 NO_3^- is highly loaded in PC3, which accounts for 13 % of the system variance. On this traverse, NO_3^-
435 in the snow has been extensively investigated, and it is proposed that NO_3^- concentrations were
436 influenced by post-depositional processing which is largely dependent on snow accumulation
437 rate (Freyer et al., 1996; Shi et al., 2015). A negative relationship was found between NO_3^- and snow
438 accumulation rate (Fig. 6(b)), suggesting a high degree of NO_3^- cycling driven by photolysis at low
439 snow accumulation sites.

440 SO_4^{2-} did not show high loadings in any of the three extracted components. Its positive loading in
441 PC1 (0.55) and weak relationships between SO_4^{2-} and sea salts (Cl^- and Na^+) likely supports the
442 contribution of sea salt aerosols, although a minor one. A positive loading of SO_4^{2-} is also present in
443 PC3 (0.42), and a weak correlation was found between SO_4^{2-} and NO_3^- . Both SO_4^{2-} (or nsSO_4^{2-}) and

444 NO_3^- are negatively correlated with snow accumulation rate (Fig. 6), but with distinct mechanisms:
445 nssSO_4^{2-} can be concentrated due to dry deposition at sites with low snow accumulation rate, while
446 elevated NO_3^- concentrations are linked to the photochemical cycling and re-deposition (discussed
447 above). In addition, nssSO_4^{2-} and NO_3^- are mainly associated with the secondary aerosols, and the
448 production of both species in summer is closely related to the oxidants HO_x , RO_x , etc, which may also
449 contribute to the correlation between SO_4^{2-} and NO_3^- .

450

4.3.2 Non-sea-salt fractions and fluxes of ions in snow pits: the non-sea-salt fractions and ion fluxes

453 In this section, we discuss the fluxes and the non-sea-salt fractions of ions at different depths (i.e.,
454 summer and winter snow) in the three snow pits. The bottom ~30 cm layer of P3 will be excluded in
455 the discussion, since it represents a snow layer clearly impacted by volcanic (Pinatubo) eruption
456 emissions.

457 Ion fluxes in snow can be determined by multiplying the concentrations by snow accumulation rate,
458 and the results in the 3 snow pits are shown in Fig. 8. The highest fluxes of ions except for NO_3^- were
459 present at P1, followed by P2 and P3. The flux of NO_3^- shows a different pattern, with the highest value
460 at P2, possibly due to the redistribution of NO_3^- across the Antarctic ice sheet driven by photolysis (Shi
461 et al., 2018b). It is noted that nssSO_4^{2-} fluxes at P1 ($99.4 \pm 46.7 \mu\text{eq m}^{-2} \text{a}^{-1}$) and P2 ($109.2 \pm 21.6 \mu\text{eq m}^{-2}$
462 a^{-1}) are comparable, although P1 is located on the coast and P2 located further inland (~800 km from
463 the coast). In addition, the ratio of nssSO_4^{2-} flux at P1 over that at P3 is 2.2, the lowest value among the
464 ratios for the observed ions (17.2, 7.5, 26.7, 8.5, 17.4, 17.0, and 10.0 for Cl^- , NO_3^- , Na^+ , NH_4^+ , K^+ ,
465 Mg^{2+} , and Ca^{2+} , respectively), suggesting more efficient transport of nssSO_4^{2-} . In other words,
466 atmospheric nssSO_4^{2-} from the open ocean can be efficiently transported to at least as far inland as
467 ~800 km from the coast (~2800 m above sea level; site P2).

468 At P1, the plots of Cl^- , K^+ , Mg^{2+} , and Ca^{2+} versus Na^+ are all close to the bulk seawater dilution line
469 (Fig. 9), with the slope values of the linear regression between Na^+ and the four ions are close to those
470 of seawater (Fig. 3), suggesting a dominant source of sea salt aerosols. The proportions of the
471 non-sea-salt fractions of K^+ , Mg^{2+} , and Ca^{2+} to the ions in snow are much lower in winter than in
472 summer, as a result of the high sea salt inputs in winter. Negative nssCl^- is present in summer snow,
473 indicating the modification to sea salts (i.e., formation of mirabilite in the atmosphere) in summer when
474 the acid levels (e.g., HNO_3) are relatively high (Savarino et al., 2007). In addition, the non-sea-salt
475 fractions of Cl^- , K^+ , Mg^{2+} , and Ca^{2+} are 0.25 ± 0.27 , 0.02 ± 0.01 , 0.04 ± 0.07 , and $0.09 \pm 0.06 \mu\text{eq L}^{-1}$,
476 respectively, contributing less to the total ion budgets. As for SO_4^{2-} in the snow, the proportion of
477 nssSO_4^{2-} to SO_4^{2-} is much higher in summer (~86%) than in winter. All nssSO_4^{2-} in summer snow is
478 positive, while some winter snow samples featured negative nssSO_4^{2-} , i.e., $\text{SO}_4^{2-}/\text{Na}^+$ ratio below the
479 value of seawater (Fig. 3S2(a)), suggesting sea salt aerosols in winter originating from the sea ice
480 (Marion et al., 1999). In the winter snow, if all of the SO_4^{2-} is from sea salt aerosols, nssSO_4^{2-} is
481 expected to be lower than or close to zero. However, 13 out of the 17 samples classified as winter snow
482 at P1 were characterized with positive nssSO_4^{2-} , suggesting a significant contribution from marine
483 biogenic emissions. It is interesting that nssSO_4^{2-} has a strong negative correlation with Na^+ in winter
484 snow ($r=0.82$, $p<0.001$), raising two potential cases: 1) stronger winds transport more sea salt aerosols
485 to P1 featured with depleted SO_4^{2-} from sea ice, thereby resulting in low concentrations of nssSO_4^{2-} and
486 assuming a stable SO_4^{2-} input flux from marine biogenic emissions; and/or 2) with a larger extent of sea
487 ice and strong transport, a large sea salt flux would still result but carry less nssSO_4^{2-} from marine

带格式的：上标

488 biogenic emissions due to the longer transport distance (Wolff et al., 2006 and references therein). If
489 case 2) dominated nssSO₄²⁻ variations in the winter snow, lower nssSO₄²⁻ would be expected in the end
490 than at the beginning of winter when a sea ice coverage minimum is present. The observation at P1,
491 however, does not support this expected seasonal trend (Fig. 3aS2). It is most likely, then, that sea salt
492 aerosol inputs dominate nssSO₄²⁻ variations in the winter snow instead of the marine biogenic
493 emissions. In addition, NH₄⁺ concentration at P1 (0.16±0.05 μeq L⁻¹) is slightly higher than the previous
494 reports of ice cores but comparable to some coastal observations (e.g., coastal sites in Terre Adelie)
495 (Legrand and Delmas, 1985; Legrand et al., 1998), possibly associated with marine biogenic emissions
496 (i.e., close to the coast) (discussed above).

497 The patterns of relationships between ions and Na⁺ at P2 are similar to those of P1 except for Ca²⁺
498 (Fig. 93). The non sea salt fractions of Cl⁻, K⁺, and Mg²⁺ at P2 are 0.42±0.18, 0.005±0.008, and
499 0.06±0.02 μeq L⁻¹, respectively, accounting for less of the total ion concentrations. nssCa²⁺, 0.13±0.01
500 μeq L⁻¹. Non-sea-salt fractions of Ca²⁺ accounts for (79±9) % of the total Ca²⁺ in snow pit P2,
501 suggesting a dominant role of the terrestrial source. Different from the other species, it is noted that
502 Ca²⁺ remains relatively constant with increasing Na⁺ (Fig. 93), possibly suggesting insignificant
503 seasonal variations in terrestrial dust inputs. As for SO₄²⁻, it is significantly enriched, and the fractions
504 of nssSO₄²⁻ to SO₄²⁻ in summer and winter snow are (94±4) and (88±4) %, respectively. The very high
505 SO₄²⁻ to Na⁺ ratio in winter (-1.6, versus 0.12 of bulk seawater), suggesting that a dominant role of
506 marine biogenic emissions dominate SO₄²⁻ other than the sea salt aerosols, different from that at P1. It
507 is suggested that the sea salt aerosol flux from the sea ice in winter is much lower in the inland
508 Antarctica than on the coast. Previous investigations proposed that sea salt aerosols emitted from sea
509 ice are an important contribution to the sea salt budget in central Antarctica in winter (Legrand et al.,
510 2016; Legrand et al., 2017b). Here, our data the high nssSO₄²⁻ concentrations indicate that marine
511 emissions could also be an important source of ions in winter.

512 At P3, Cl⁻, K⁺, and Mg²⁺ are also correlated well with Na⁺ (Fig. 93), and the non sea salt fractions of
513 the 3 ions are 0.58±0.34, 0.02±0.01, and 0.12±0.04 μeq L⁻¹, respectively, higher than those of P2. The
514 non-sea-salt fractions of Cl⁻ make up (38±24) % of the total, similar to that at P2, indicating. Although
515 the sea salt fractions of Cl⁻, K⁺, and Mg²⁺ account for most of their total budgets in the snow, the other
516 sources can occasionally be important. On average, nssCl⁻ accounts for 40 % of the total Cl⁻,
517 suggesting that Cl⁻ at Dome A is mainly from the sea salt aerosols, but the importance of HCl
518 deposition, and consequently results in Cl⁻ not being a quantitative indicator of sea salts in the interior
519 areas. of HCl is also an important contribution. This percentage is higher than that at P2 (~30 %),
520 suggesting a more important role of HCl on Cl⁻ budget in further inland snow. At P3, nssCa²⁺ accounts
521 for % of total Ca²⁺, close to that of P2, suggesting the terrestrial particle mass as the primary source.
522 In terms of nssSO₄²⁻, at P3 the non sea salt fraction accounts for ~(95±2) % of total SO₄²⁻,
523 comparable to that of P2. Together with the observations at P2. At P2 and P3, it can be inferred that SO₄²⁻
524 in both summer and winter snow in the interior areas is dominated by marine biogenic emissions
525 throughout the year (i.e., no negative nssSO₄²⁻ observed), generally in line with the observation at
526 Dome C (Udisti et al., 2012).

527 Ion fluxes in the 3 snow pits can be determined by multiplying the concentrations by snow
528 accumulation rate, and the highest fluxes of ions except for NO₃⁻ were generally present at P1, followed
529 by P2 and P3 (Fig. S5). It is noted that nssSO₄²⁻ fluxes at P1 (99.4±46.7 μeq m⁻² a⁻¹) and P2
530 (109.2±21.6 μeq m⁻² a⁻¹) are comparable, although P1 is located on the coast and P2 located further
531 inland (~800 km from the coast). In addition, the ratio of nssSO₄²⁻ flux at P1 over that at P3 is 2.2, the

带格式的：上标

532 lowest among the ratios for the observed ions (17.2, 7.5, 26.7, 8.5, 17.4, 17.0, and 10.0 for Cl^- , NO_3^- ,
533 Na^+ , NH_4^+ , K^+ , Mg^{2+} , and Ca^{2+} , respectively), suggesting more efficient transport of nssSO_4^{2-} . In other
534 words, atmospheric nssSO_4^{2-} from the open ocean can be efficiently transported to at least as far inland
535 as ~800 km from the coast (~2800 m above sea level; site P2).

536 Similar to the surface snow, the modification processes to sea salt aerosols is negligible in snow pit
537 P1, while the ubiquitous modification process to sea salts throughout the year was found in the interior
538 areas (P2 and P3; Fig. S3). Thus, Cl^- in inland Antarctica, often deviating from the seawater dilution
539 line remarkably in both summer and winter, is not a quantitative indicator of sea salts in snow.

540

541 5 Conclusions

542 ~~Snow chemistry~~ Surface snow and snow pit samples collected on a traverse from coastal Zhongshan
543 Station to the ice sheet summit Dome A, East Antarctica, during five campaigns were used to
544 comprehensively investigate spatial and temporal variations in snow chemistry. It is shown that
545 the non-sea-salt fractions of K^+ , Mg^{2+} , and Ca^{2+} are mainly associated with terrestrial particle mass,
546 while nssCl^- is linked to the deposition of HCl. Spatially, the proportions of non-sea-salt fractions of
547 ions to the totals are higher in the interior areas than on the coast, and seasonally, the proportions are
548 generally higher in summer than in winter, due to the high sea salt inputs during wintertime. Negative
549 nssSO_4^{2-} observed on the coast indicates sea salts mainly originating from the sea ice in winter, while
550 positive nssSO_4^{2-} is present throughout the year in the interior areas, suggesting the dominated role of
551 marine biogenic emissions. The nssSO_4^{2-} can be transported efficiently to at least as far inland as the
552 ~2800 m contour line.

553 Cl^- , Na^+ , K^+ , and Mg^{2+} concentrations are high within the narrow coastal region, falling off strongly
554 further inland, while NO_3^- exhibits an opposite trend and no clear spatial trends were found for SO_4^{2-} ,
555 NH_4^+ , and Ca^{2+} . In inland snow, Cl^- , K^+ , and Mg^{2+} are slightly enriched relative to Na^+ with respect to
556 the composition of seawater. nssCl^- is associated with the deposition of HCl produced from
557 dechlorination of sea salt aerosols, and nssK^+ and nssMg^{2+} are possibly linked to terrestrial particle
558 mass. Ca^{2+} and SO_4^{2-} are significantly enriched versus Na^+ , and terrestrial dust mass and marine
559 biogenic emissions are responsible for the enrichments respectively. Snow NH_4^+ is related to marine
560 biological activities, and multivariate statistical analysis suggests, at least in part, the NH_4^+ transport is
561 via free troposphere.

562 On the coast, parts of the winter snow showed a depletion of SO_4^{2-} versus Na^+ , indicating sea salt
563 aerosols sourced from sea ice. In the interior areas, SO_4^{2-} in both summer and winter snow is dominated
564 by marine biogenic emissions, with no negative nssSO_4^{2-} values observed. In general, the contribution
565 proportions of nssCl^- to total Cl^- are higher in interior snow than in coastal snow. Ternary plots of Cl^- ,
566 Na^+ , and SO_4^{2-} in snow suggest the modification process to sea salts is negligible on the coast, while
567 the degree of modification to sea salts is higher in inland throughout the year, which results in Cl^- not
568 being a quantitative indicator of sea salts. Ion flux assessment suggests an efficient transport of
569 nssSO_4^{2-} to at least as far inland as the ~2800 m contour line.

570

571 **Data availability.** This dataset, chemical data on ion concentrations in snow on the traverse from coast
572 (Zhongshan Station) to Dome A, is in the process of being hosted on a public server by the Chinese
573 National Arctic and Antarctic Data Center (<https://www.chinare.org.cn/>).

574

575 **Author contributions.** GS, ZC, YL and BS designed the experiments and GS, HM, ZH, CA, SJ, TM,

576 JY, DW and SL carried them out. GS and MH prepared the manuscript with contributions from all
577 co-authors.

578

579 **Competing interests.** The authors declare that they have no conflict of interest.

580

581 **Acknowledgements**

582 This research was supported by the National Science Foundation of China (Grant Nos. 41922046 and
583 41576190 to GS; Grant No. 41876225 to HM) and the National Key Research and Development
584 Program of China (Grant Nos. 2016YFA0302204 and 2019YFC1509102 to GS). The authors are
585 grateful to the CHINARE inland members for logistic support and assistance.

586

587 **References**

- 588 Bertler, N., Mayewski, P.A., Aristarain, A., Barrett, P., Becagli, S., Bernardo, R., Bo, S., Xiao, C.,
589 Curran, M., and Qin, D.: Snow chemistry across Antarctica, *Ann. Glaciol.*, 41, 167-179, 2005.
- 590 Bondietti, E.A., and Papastefanou, C.: Estimates of residence times of sulfate aerosols in ambient air,
591 *Sci. Total Environ.*, 136, 25-31, doi:10.1016/0048-9697(93)90294-G, 1993.
- 592 Ding, M., Xiao, C., Li, Y., Ren, J., Hou, S., Jin, B., and Sun, B.: Spatial variability of surface mass
593 balance along a traverse route from Zhongshan station to Dome A, Antarctica, *J. Glaciol.*, 57, 658-666,
594 2011.
- 595 Dixon, D.A., Mayewski, P.A., Korotkikh, E., Sneed, S.B., Handley, M.J., Introne, D.S., and Scambos,
596 T.A.: Variations in snow and firn chemistry along US ITASE traverses and the effect of surface glazing,
597 *Cryosphere*, 7, 515-535, doi:10.5194/tc-7-515-2013, 2013.
- 598 Du, Z., Xiao, C., Ding, M., and Li, C.: Identification of multiple natural and anthropogenic sources of
599 dust in snow from Zhongshan Station to Dome A, East Antarctica, *J. Glaciol.*, 64, 855-865,
600 doi:10.1017/jog.2018.72, 2018.
- 601 Du, Z., Xiao, C., Handley, M.J., Mayewski, P.A., Li, C., Liu, S., Ma, X., and Yang, J.: Fe variation
602 characteristics and sources in snow samples along a traverse from Zhongshan Station to Dome A, East
603 Antarctica, *Sci. Total Environ.*, doi:https://doi.org/10.1016/j.scitotenv.2019.04.139, 2019.
- 604 Finlayson-Pitts, B.J.: The tropospheric chemistry of sea salt: a molecular-level view of the chemistry of
605 NaCl and NaBr, *Chem. Rev.*, 103, 4801-4822, 2003.
- 606 Gragnani, R., Smiraglia, C., Stenni, B., and Torcini, S.: Chemical and isotopic profiles from snow pits
607 and shallow firn cores on Campbell Glacier, northern Victoria Land, Antarctica, *Ann. Glaciol.*, 27,
608 679-684, 1998.
- 609 Hara, K., Nakazawa, F., Fujita, S., Fukui, K., Enomoto, H., and Sugiyama, S.: Horizontal distributions
610 of aerosol constituents and their mixing states in Antarctica during the JASE traverse, *Atmos. Chem.*
611 *Phys.*, 14, 10211-10230, doi:10.5194/acp-14-10211-2014, 2014.
- 612 Hara, K., Osada, K., and Yamanouchi, T.: Tethered balloon-borne aerosol measurements: seasonal and
613 vertical variations of aerosol constituents over Syowa Station, Antarctica, *Atmos. Chem. Phys.*, 13,
614 9119-9139, 2013.
- 615 Hou, S., Li, Y., Xiao, C., and Ren, J.: Recent accumulation rate at Dome A, Antarctica, *Chin. Sci. Bull.*,
616 52, 428-431, 2007.
- 617 Keene, W.C., Maring, H., Maben, J.R., Kieber, D.J., Pszenny, A.A., Dahl, E.E., Izaguirre, M.A., Davis,
618 A.J., Long, M.S., and Zhou, X.: Chemical and physical characteristics of nascent aerosols produced by

619 bursting bubbles at a model air - sea interface, *J. Geophys. Res.*, 112, D21202,
620 doi:10.1029/2007JD008464, 2007.

621 Khodzher, T.V., Golobokova, L.P., Osipov, E.Y., Shibaev, Y.A., Lipenkov, V.Y., Osipova, O.P., and Petit,
622 J.R.: Spatial-temporal dynamics of chemical composition of surface snow in East Antarctica along the
623 Progress station-Vostok station transect, *Cryosphere*, 8, 931–939, doi:10.5194/tc-8-931-2014, 2014.

624 Legrand, M.: Chemistry of Antarctic snow and ice, *J. de Phys.*, 48, 77-86, 1987.

625 Legrand, M., and Delmas, R.J.: Spatial and temporal variations of snow chemistry in Terre Adélie (East
626 Antarctica), *Ann. Glaciol.*, 7, 20-25, 1985.

627 Legrand, M., Preunkert, S., Weller, R., Zipf, L., Elsässer, C., Merchel, S., Rugel, G., and Wagenbach,
628 D.: Year-round record of bulk and size-segregated aerosol composition in central Antarctica (Concordia
629 site) – Part 2: Biogenic sulfur (sulfate and methanesulfonate) aerosol, *Atmos. Chem. Phys.*, 17,
630 14055-14073, doi:10.5194/acp-17-14055-2017, 2017a.

631 Legrand, M., Preunkert, S., Wolff, E., Weller, R., Jourdain, B., and Wagenbach, D.: Year-round records
632 of bulk and size-segregated aerosol composition in central Antarctica (Concordia site) – Part 1:
633 Fractionation of sea-salt particles, *Atmos. Chem. Phys.*, 17, 14039-14054,
634 doi:10.5194/acp-17-14039-2017, 2017b.

635 Legrand, M., Yang, X., Preunkert, S., and Theys, N.: Year-round records of sea salt, gaseous, and
636 particulate inorganic bromine in the atmospheric boundary layer at coastal (Dumont d'Urville) and
637 central (Concordia) East Antarctic sites, *J. Geophys. Res.*, 121, 2015JD024066,
638 doi:10.1002/2015JD024066, 2016.

639 Li, C., Xiao, C., Shi, G., Ding, M., Qin, D., and Ren, J.: Spatial and temporal variability of
640 marine-origin matter along a transect from Zhongshan Station to Dome A, Eastern Antarctica, *J.*
641 *Environ. Sci.*, 46, 190-202, doi:10.1016/j.jes.2015.07.011, 2016.

642 Marion, G., Farren, R., and Komrowski, A.: Alternative pathways for seawater freezing, *Cold Reg. Sci.*
643 *Technol.*, 29, 259-266, 1999.

644 Mayewski, P.A., Carleton, A.M., Birkel, S.D., Dixon, D., Kurbatov, A.V., Korotkikh, E., McConnell, J.,
645 Curran, M., Cole-Dai, J., Jiang, S., Plummer, C., Vance, T., Maasch, K.A., Sneed, S.B., and Handley,
646 M.: Ice core and climate reanalysis analogs to predict Antarctic and Southern Hemisphere climate
647 changes, *Quaternary Sci. Rev.*, 155, 50-66, doi:https://doi.org/10.1016/j.quascirev.2016.11.017, 2017.

648 Mulvaney, R., and Wolff, E.: Spatial variability of the major chemistry of the Antarctic ice sheet, *Ann.*
649 *Glaciol.*, 20, 440-447, 1994.

650 Neubauer, J., and Heumann, K.G.: Nitrate trace determinations in snow and firn core samples of ice
651 shelves at the Weddell Sea, Antarctica, *Atmospheric Environment (1967)*, 22, 537-545, 1988.

652 Proposito, M., Becagli, S., Castellano, E., Flora, O., Genoni, L., Gagnani, R., Stenni, B., Traversi, R.,
653 Udisti, R., and Frezzotti, M.: Chemical and isotopic snow variability along the 1998 ITASE traverse
654 from Terra Nova Bay to Dome C, East Antarctica, *Ann. Glaciol.*, 35, 187-194, 2002.

655 Qin, D., Zeller, E.J., and Dreschhoff, G.A.: The distribution of nitrate content in the surface snow of the
656 Antarctic Ice Sheet along the route of the 1990 International Trans-Antarctica Expedition, *J. Geophys.*
657 *Res.*, 97, 6277-6284, 1992.

658 Rankin, A.M., and Wolff, E.W.: Ammonium and potassium in snow around an emperor penguin colony,
659 *Antarct. Sci.*, 12, 154-159, doi:10.1017/S0954102000000201, 2000.

660 Russell, A., and McGregor, G.R.: Southern hemisphere atmospheric circulation: impacts on Antarctic
661 climate and reconstructions from Antarctic ice core data, *Climatic. Change*, 99, 155-192, 2010.

662 Savarino, J., Kaiser, J., Morin, S., Sigman, D.M., and Thiemens, M.H.: Nitrogen and oxygen isotopic

663 constraints on the origin of atmospheric nitrate in coastal Antarctica, *Atmos. Chem. Phys.*, 7,
664 1925-1945, 2007.

665 Severi, M., Becagli, S., Castellano, E., Morganti, A., Traversi, R., and Udisti, R.: Thirty years of snow
666 deposition at Talos Dome (Northern Victoria Land, East Antarctica): Chemical profiles and climatic
667 implications, *Microchem. J.*, 92, 15-20, doi:<https://doi.org/10.1016/j.microc.2008.08.004>, 2009.

668 Shi, G., Buffen, A.M., Hastings, M.G., Li, C., Ma, H., Li, Y., Sun, B., An, C., and Jiang, S.:
669 Investigation of post-depositional processing of nitrate in East Antarctic snow: isotopic constraints on
670 photolytic loss, re-oxidation, and source inputs, *Atmos. Chem. Phys.*, 15, 9435–9453,
671 doi:[10.5194/acp-15-9435-2015](https://doi.org/10.5194/acp-15-9435-2015), 2015.

672 Shi, G., Buffen, A.M., Ma, H., Hu, Z., Sun, B., Li, C., Yu, J., Ma, T., An, C., Jiang, S., Li, Y., and
673 Hastings, M.G.: Distinguishing summertime atmospheric production of nitrate across the East Antarctic
674 Ice Sheet, *Geochim. Cosmochim. Acta*, 231, 1-14, doi:[10.1016/j.gca.2018.03.025](https://doi.org/10.1016/j.gca.2018.03.025), 2018.

675 Shi, G., Li, Y., Jiang, S., An, C., Ma, H., Sun, B., and Wang, Y.: Large-scale spatial variability of major
676 ions in the atmospheric wet deposition along the China Antarctica transect (31° N~ 69° S), *Tellus B*, 64,
677 17134, doi:[10.3402/tellusb.v64i0.17134](https://doi.org/10.3402/tellusb.v64i0.17134), 2012.

678 Sigl, M., Fudge, T.J., Winstrup, M., Cole-Dai, J., Ferris, D., McConnell, J.R., Taylor, K.C., Welten, K.C.,
679 Woodruff, T.E., Adolphi, F., Bisiaux, M., Brook, E.J., Buizert, C., Caffee, M.W., Dunbar, N.W.,
680 Edwards, R., Geng, L., Iverson, N., Koffman, B., Layman, L., Maselli, O.J., McGwire, K., Muscheler,
681 R., Nishiizumi, K., Pasteris, D.R., Rhodes, R.H., and Sowers, T.A.: The WAIS Divide deep ice core
682 WD2014 chronology - Part 2: Annual-layer counting (0-31 ka BP), *Clim. Past*, 12, 769-786,
683 doi:[10.5194/cp-12-769-2016](https://doi.org/10.5194/cp-12-769-2016), 2016.

684 Suzuki, T., Iizuka, Y., Matsuoka, K., Furukawa, T., Kamiyama, K., and Watanabe, O.: Distribution of
685 sea salt components in snow cover along the traverse route from the coast to Dome Fuji station 1000
686 km inland at east Dronning Maud Land, Antarctica, *Tellus B Chemical and Physical Meteorology*, 54,
687 407-411, 2002.

688 Traversi, R., Becagli, S., Castellano, E., Largiuni, O., Migliori, A., Severi, M., Frezzotti, M., and Udisti,
689 R.: Spatial and temporal distribution of environmental markers from Coastal to Plateau areas in
690 Antarctica by firn core chemical analysis, *Int. J. Environ. Anal. Chem.*, 84, 457-470,
691 doi:[10.1080/03067310310001640393](https://doi.org/10.1080/03067310310001640393), 2004.

692 Udisti, R., Dayan, U., Becagli, S., Busetto, M., Frosini, D., Legrand, M., Lucarelli, F., Preunkert, S.,
693 Severi, M., and Traversi, R.: Sea spray aerosol in central Antarctica. Present atmospheric behaviour and
694 implications for paleoclimatic reconstructions, *Atmos. Environ.*, 52, 109-120,
695 doi:[10.1016/j.atmosenv.2011.10.018](https://doi.org/10.1016/j.atmosenv.2011.10.018), 2012.

696 Virkkula, A., Teinilä, K., Hillamo, R., Kerminen, V.M., Saarikoski, S., Aurela, M., Koponen, I.K., and
697 Kulmala, M.: Chemical size distributions of boundary layer aerosol over the Atlantic Ocean and at an
698 Antarctic site, *Atmos. Chem. Phys.*, 6, 303-310, 2006.

699 Wagenbach, D., Ducroz, F., Mulvaney, R., Keck, L., Minikin, A., Legrand, M., Hall, J.S., and Wolff,
700 E.W.: Sea-salt aerosol in coastal Antarctic regions, *J. Geophys. Res.*, 103, 10961-10974, 1998.

701 Weller, R., Wagenbach, D., Legrand, M., Elsässer, C., Tian-kunze, X., and Königlanglo, G.: Continuous
702 25-yr aerosol records at coastal Antarctica-: inter-annual variability of ionic compounds and links to
703 climate indices, *Tellus B*, 63, 901-919, doi:[10.1111/j.1600-0889.2011.00542.x](https://doi.org/10.1111/j.1600-0889.2011.00542.x), 2011.

704 Wolff, E.W., Barbante, S., Becagle, S., Bigler, M., Boutron, C.F., Castellano, E., de Angelis, M., and
705 Federer, U.: Changes in environment over the last 800,000 years from chemical analysis of the EPICA
706 Dome C ice core, *Quaternary Sci. Rev.*, 29, 285-295, 2010.

707 Wolff, E.W., Fischer, H., Fundel, F., Ruth, U., Twarloh, B., Littot, G.C., Mulvaney, R., Röthlisberger,
708 R., de Angelis, M., Boutron, C.F., Hansson, M., Jonsell, U., Hutterli, M.A., Lambert, F., Kaufmann, P.,
709 Stauffer, B., Stocker, T.F., Steffensen, J.P., Bigler, M., Siggaard-Andersen, M.L., Udisti, R., Becagli, S.,
710 Castellano, E., Severi, M., Wagenbach, D., Barbante, C., Gabrielli, P., and Gaspari, V.: Southern Ocean
711 sea-ice extent, productivity and iron flux over the past eight glacial cycles, *Nature*, 440, 491-496,
712 doi:10.1038/nature04614, 2006.
713
714

715 **Table 1** Rotated component matrix of the major ions in surface snow. (Extraction method: principal
 716 component analysis. Rotation method: varimax with Kaiser normalization. Rotation converged in 4
 717 iterations.) Factor loadings were calculated from the eigenvalues of the three components and their
 718 corresponding eigenvectors, and the values greater than 0.7 are shaded.

Chemical ions	PC1	PC2	PC3	Communalities
Cl ⁻	0.93	-0.01	0.27	0.93
NO ₃ ⁻	0.04	-0.06	0.95	0.90
SO ₄ ²⁻	0.55	0.08	0.42	0.49
Na ⁺	0.98	-0.01	-0.06	0.96
NH ₄ ⁺	0.10	0.81	0.04	0.66
K ⁺	0.71	0.25	0.12	0.57
Mg ²⁺	0.96	0.05	-0.09	0.92
Ca ²⁺	0.03	0.79	-0.07	0.62
Initial eigenvalues	3.67	1.33	1.06	
Percentage of variance	46	17	13	
Cumulative percent	46	63	76	

719

720

721 **Table 2** Pearson correlation matrix of major ions in surface snow

—	Cl ⁻	NO ₃ ⁻	SO ₄ ²⁻	Na ⁺	NH ₄ ⁺	K ⁺	Mg ²⁺	Ca ²⁺
Cl ⁻	1.00	0.24 ^{**}	0.47 ^{**}	0.94 ^{**}	0.05	0.74 ^{**}	0.91 ^{**}	0.09
NO ₃ ⁻		1.00	0.21 ^{**}	-0.02	-0.04	0.09 [*]	-0.04	-0.05
SO ₄ ²⁻			1.00	0.34 ^{**}	0.08	0.30 ^{**}	0.31 ^{**}	0.03
Na ⁺				1.00	0.05	0.77 ^{**}	0.98 ^{**}	0.12 [*]
NH ₄ ⁺					1.00	0.19 ^{**}	0.10 [*]	0.30 ^{**}
K ⁺						1.00	0.75 ^{**}	0.15 ^{**}
Mg ²⁺							1.00	0.15 ^{**}
Ca ²⁺								1.00

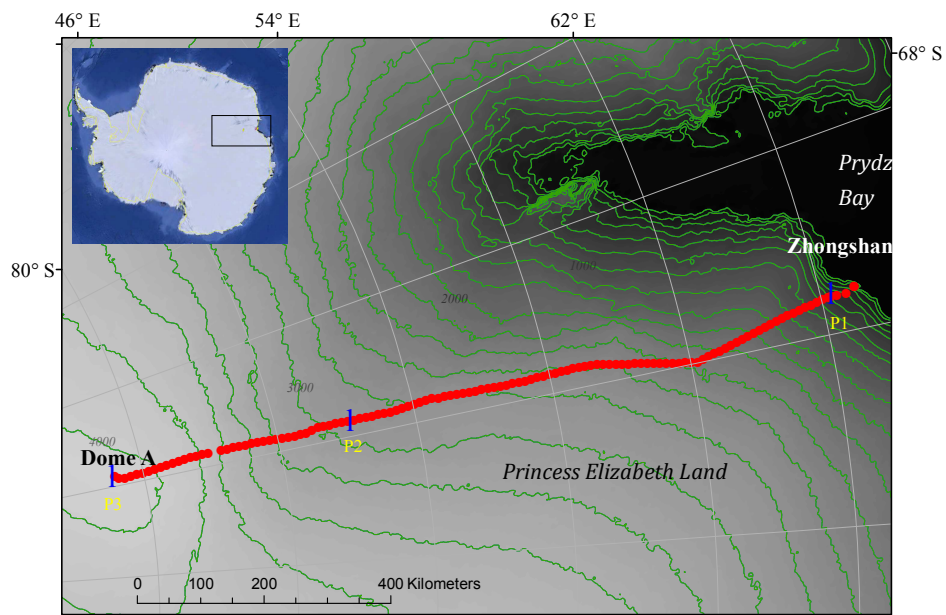
722 ^{**}-Correlation is significant at the 0.01 level (2-tailed).

723 ^{*}-Correlation is significant at the 0.05 level (2-tailed).

724

725

726

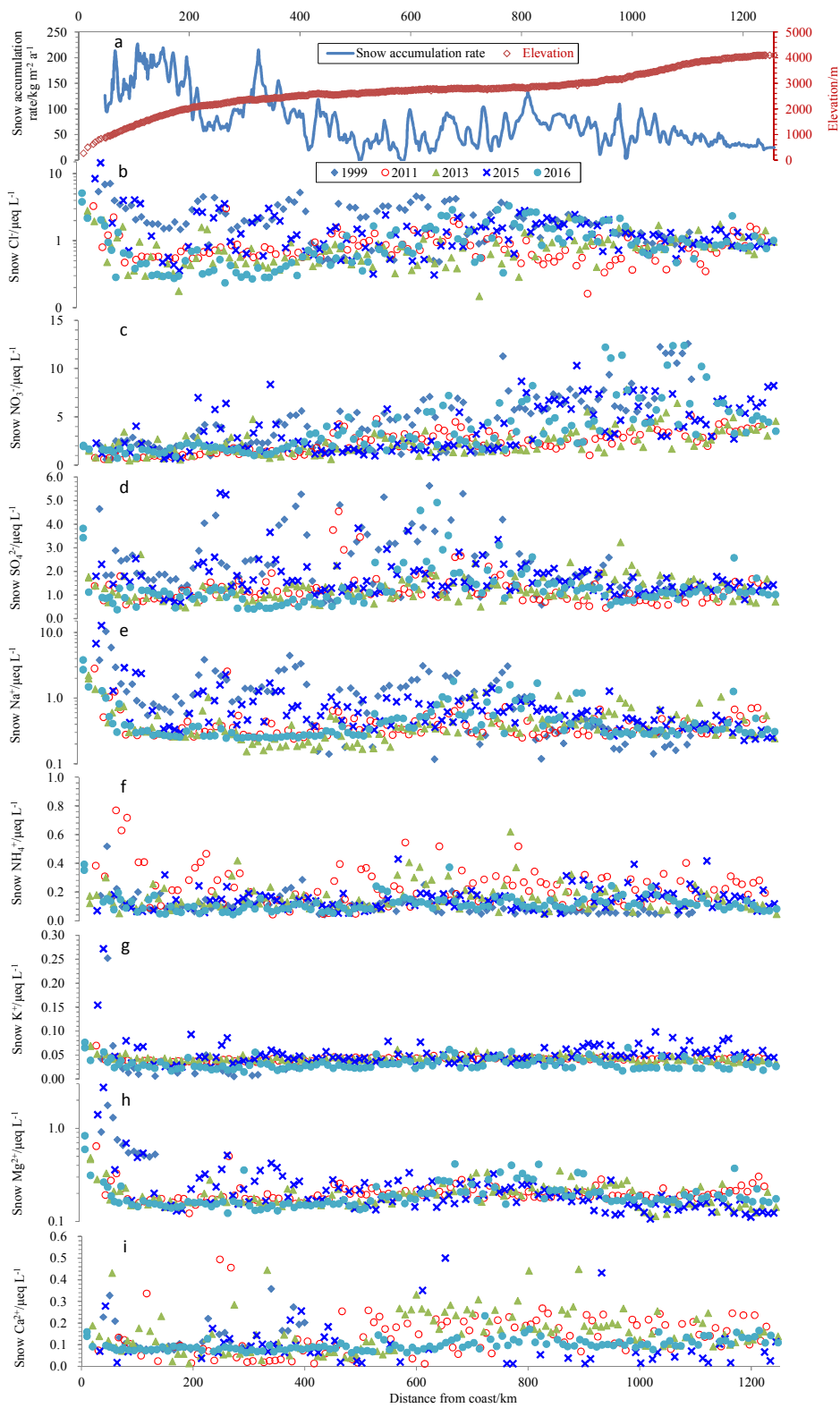


727

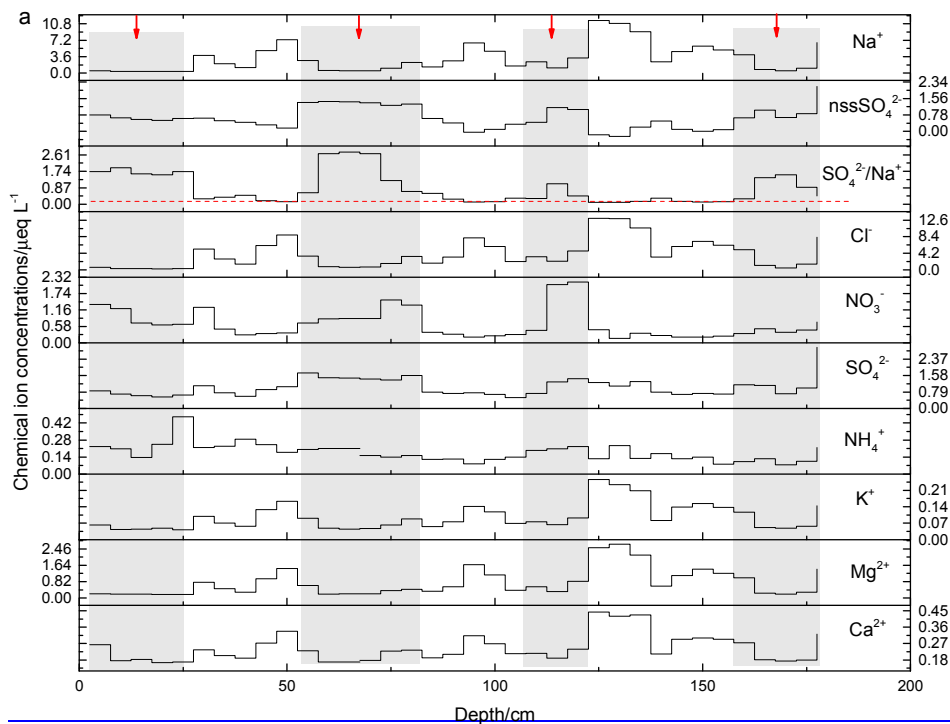
728

729

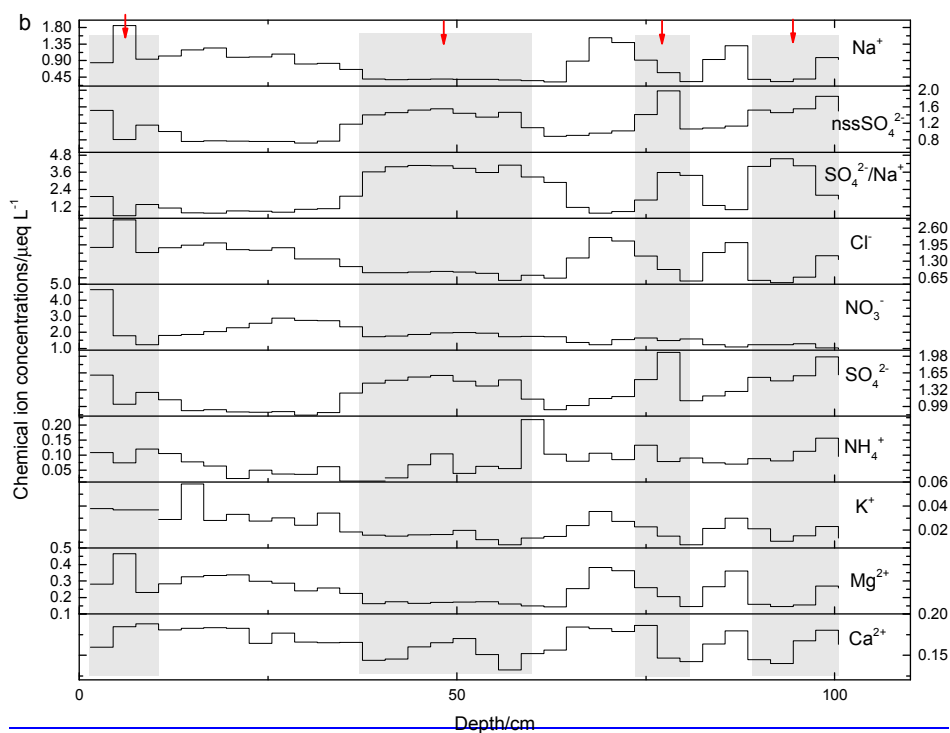
Figure 1. The Chinese inland investigation traverse from the coast (Zhongshan station) to the ice sheet summit, Dome A, East Antarctica. The traverse is generally along the 77.0°E longitude.



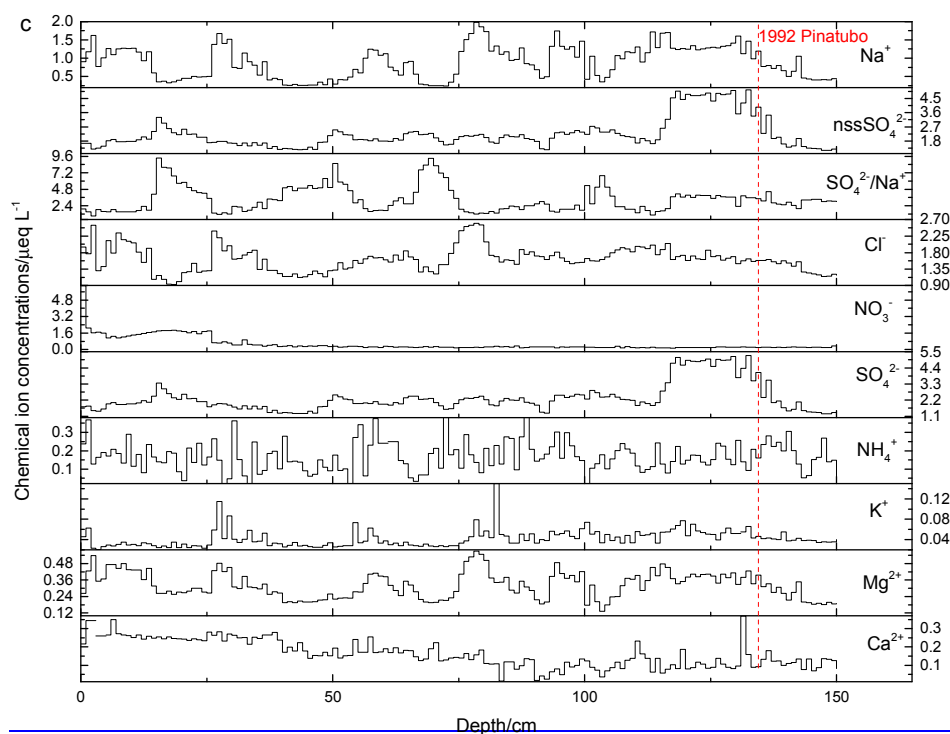
731 | **Figure 2.1.** Annual snow accumulation rate, elevation (a) and ion concentrations in surface snow
 732 | collected during five seasons (b-i). Annual snow accumulation rate is obtained from field bamboo stick
 733 | measurements, updated to 2016 from Ding et al. (2011). The closed diamond, open circle, closed
 734 | triangle, cross and closed circle denote ion concentrations in the years 1999, 2011, 2013, 2015, and
 735 | 2016, respectively. Note that a base-10 log scale is used for the y-axis of Cl^- (b), Na^+ (e), and Mg^{2+} (h).
 736 |



737 |



738



739

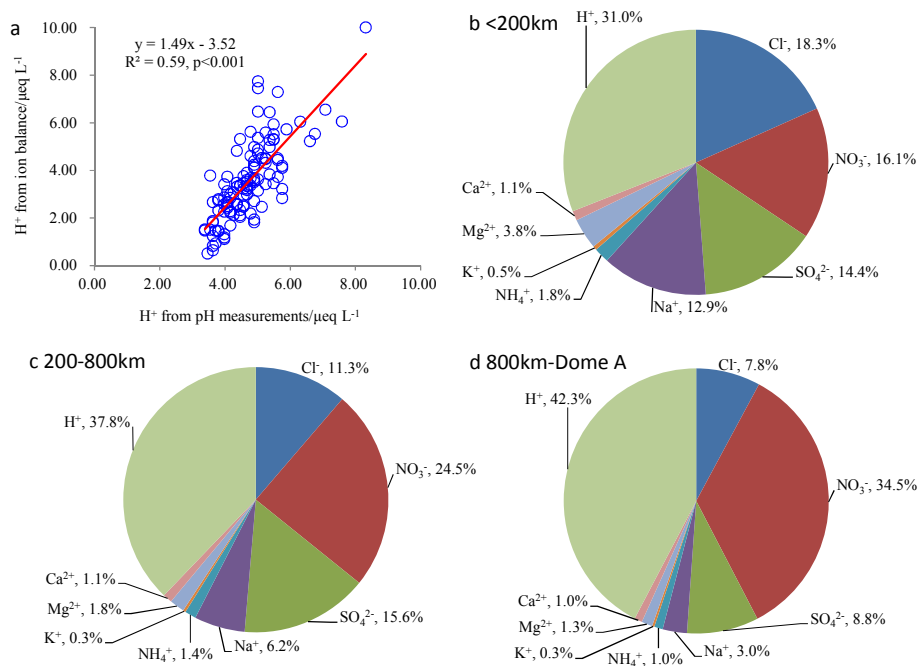
740

741

Figure 3. Profiles of chemical ions in snow pits P1 (a), P2 (b), and P3 (c). Snow pits P1 and P2 were sampled in the summer season in 2015-2016, and P3 was sampled in January 2010. The ratios of

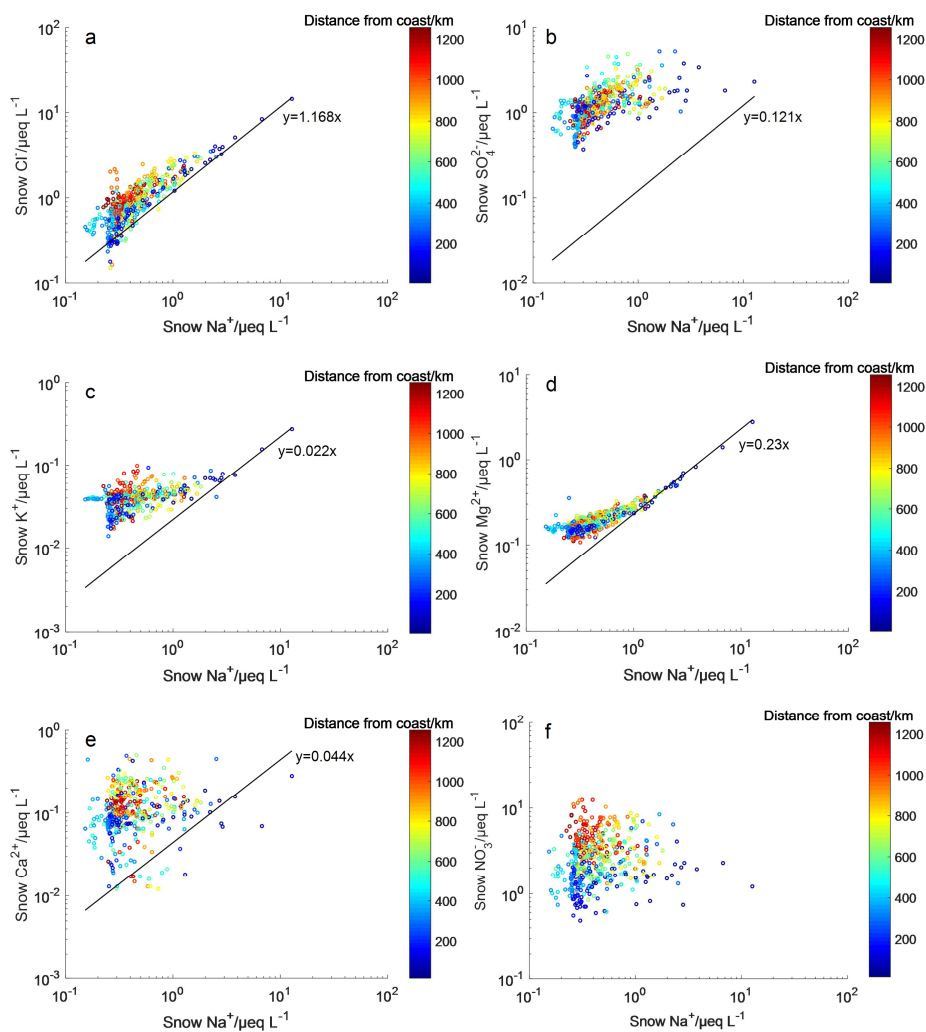
742 | $\text{SO}_4^{2-}/\text{Na}^+$ in snow samples were also present. Red arrows in panels (a) and (b) represent the middle of
743 | the identified summer, and shaded areas denote summer seasons (see text). The red dashed line in panel
744 | (a) represents the ratio of $\text{SO}_4^{2-}/\text{Na}^+$ in bulk seawater, while the red dashed line in panel (c) signifies the
745 | first snow sample significantly influenced by the Pinatubo eruption. One seasonal cycle generally
746 | represents local Na^+ minima and SO_4^{2-} and $\text{SO}_4^{2-}/\text{Na}^+$ maxima.
747 | _____

748
749
750



751
752
753
754
755
756
757

Figure 4. Major ions in surface snow on the Chinese inland Antarctic traverse. Concentrations of H^+ derived from pH versus those from the ion balance method are shown in panel (a), and contribution percentages of each ion to the total in different regions on the traverse are shown in panels (b)–(d), in $\mu\text{eq L}^{-1}$. The percentages of each ion in individual regions were calculated from the averages of all sites within the region.

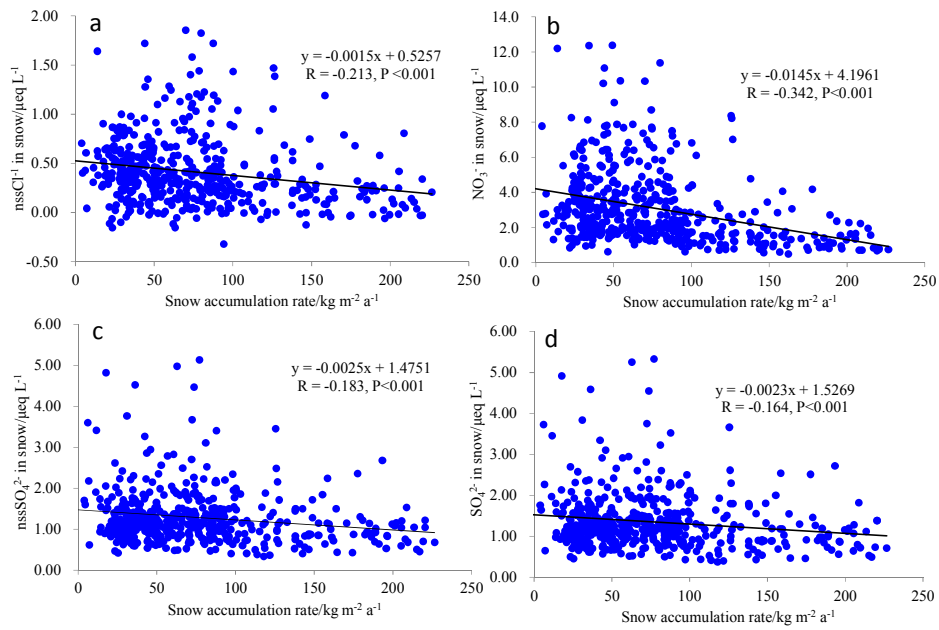


758

759 | **Figure 52.** Correlation plots of Cl^- , SO_4^{2-} , K^+ , Mg^{2+} , Ca^{2+} , and NO_3^- versus Na^+ in surface snow. The
 760 black solid line represents the seawater dilution line, with slopes of typical ions versus Na^+ ratios in
 761 seawater (in $\mu\text{eq L}^{-1}$). The concentration of NO_3^- in seawater is too variable among the seas, and a
 762 representative ratio of $\text{NO}_3^-/\text{Na}^+$ cannot be presented. Note that a base-10 log scale is used for ion
 763 concentrations.

764

765



766

767

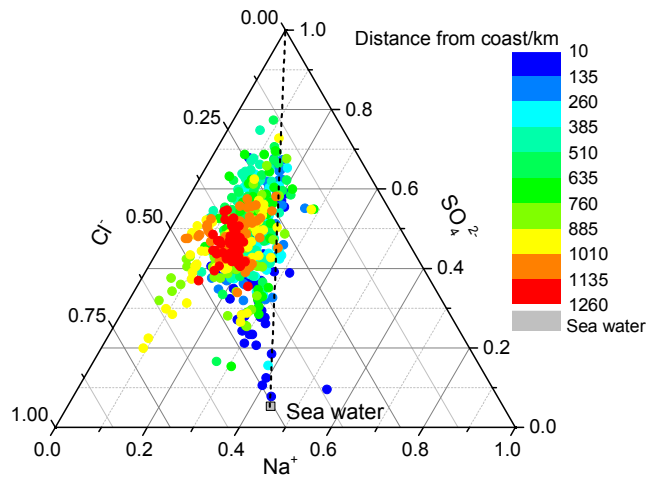
Figure 6. Relationship between chemical ions in surface snow and snow accumulation rate on the traverse.

768

769

770

771

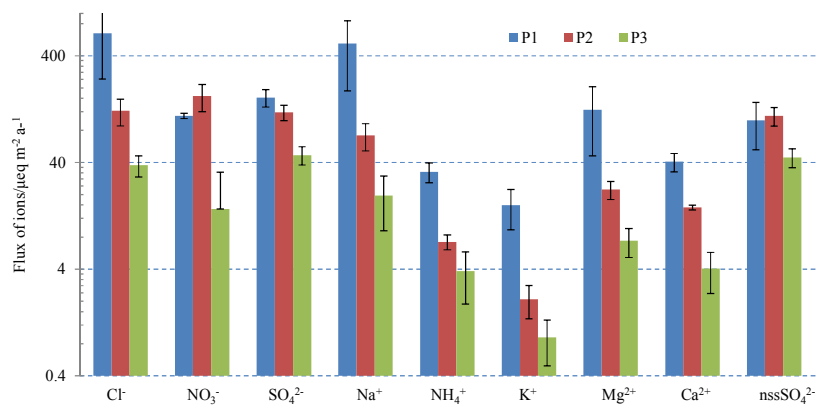


772

773 **Figure 7.** Ternary plot of Cl^- , Na^+ , and SO_4^{2-} in surface snow samples. Bulk seawater composition is
774 denoted by a grey square. The dashed line extending between the sea salt reference value and the SO_4^{2-}
775 summit represents the composition of sea salt with increasing SO_4^{2-} .

776

777



778

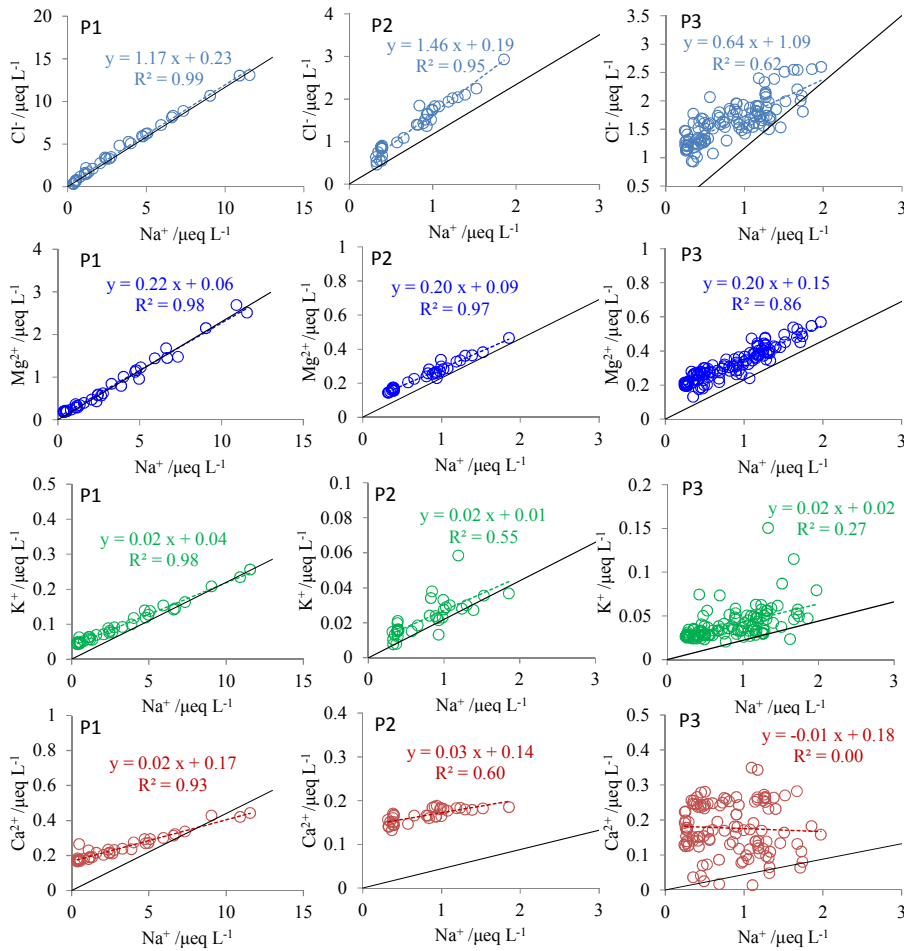
779

780

781

Figure 8. Ion fluxes at the three pits (P1, P2, and P3). The error bars represent one standard deviation of fluxes in different years. Note that a base-10 log scale is used for the y-axis.

782



783

784 **Figure 93.** Relationships between Na⁺ and Cl⁻, K⁺, Mg²⁺, Ca²⁺ in the three snow pits (P1, P2, and P3).
 785 Also shown are the linear regressions between them (dashed line), with all of the linear correlation
 786 significant at p<0.001 except Ca²⁺/Na⁺ at P3. The black solid line represents seawater dilution line.
 787 Note that the data of the bottom ~30 cm layer of P3 was excluded in the plots, since it represents a
 788 snow layer clearly impacted by volcanic (Pinatubo) eruption emissions.
 789